On The Diffusion of Sticky Particles in 1-D

Joshua DM Hellier* and Graeme J Ackland†
SUPA, School of Physics and Astronomy, University of Edinburgh, Mayfield Road, Edinburgh EH9 3JZ, United Kingdom
(Dated: May 15, 2018)

The 1D Ising model is the simplest Hamiltonian-based model in statistical mechanics. The simplest interacting particle process is the Symmetric Exclusion Process (SEP), a 1D lattice gas of particles that hop symmetrically and cannot overlap. Combining the two gives a model for sticky particle diffusion, SPM, which is described here. SPM dynamics are based on SEP with short-range interaction, allowing flow due to non-equilibrium boundary conditions. We prove that SPM is also a detailed-balance respecting, particle-conserving, Monte Carlo description of the Ising model. Neither the Ising model nor SEP have a phase transition in 1D, but the SPM exhibits a non-equilibrium transition. This is from normal diffusion to a state with close to zero flow, breaking into a two-phase mixture. We present a fully non-linear, analytic, mean-field solution, which has a crossover from a positive to a negative diffusion constant coincident with the full SPM transition. Thus the mean field theory successfully predicts its own demise. The simplicity of the model suggests a wide range of possible applications.

Lattice gases are a ubiquitous tool for modeling complex systems from biology to traffic [1–7]. Analytically solvable cases involve non-interacting or excluding particles, but in any real system of interest the moving objects interact. Many models tackle the situation where the diffusing objects interact with an external field of the substrate [8–13], and non-trivial flow is induced by these non-equilibrium interactions.

For many applications, one is interested in a system where the only non-equilibrium feature is a driving force applied at the boundaries, such as a chemical potential difference, while away from the boundaries the system is free to self-organise. There is surprisingly little work considering how complex flow arises only interactions between the moving particles themselves, allowing the system to self-organise according to some equilibrium. One reason for this is that the interactions introduce nonlinearities in analytical models, which makes them challenging to solve, at least outside of limits in which they can be linearized. This is unfortunate because it is precisely these nonlinearities which introduce interesting behaviors such as discontinuities at the oxide-metal interface or diffusion instability [14, 15].

Here we investigate a simple one-dimensional model, the "Sticky Particle Model" or SPM, specified in the top left inset of Fig. 1, which contains such interparticle interactions. We explore the impact this has on particle-flow, in particular when observed in the large-scale limit.

There are many examples of models of driven-dissipative dynamics, it is sometimes assumed that locally non-equilibrium dynamics are required to model complex flows. The novel feature of SPM is that it has locally equilibrium dynamics (i.e. obeys detailed balance) but still exhibits a nonequilibrium phase transformation from a homogeneous, diffusing phase to a jammed structure. It demonstrates that while local dissipation or substrate interactions can cause non-diffusive flow, they are not a necessary requirement.

One might contrast this approach (making a simple microscopic model and trying to learn from it about large-scale interface growth) with approaches such as the KPZ equation [16–18] (where one analyses the extreme large-scale dynamics using universality classes).

The SPM is based upon the symmetric exclusion process [19–24], augmented by an interaction rule that adjacent particles separate with rate λ instead of their normal hopping rate, 1. It is equivalent to the KLS model [25–27] in 1-dimension without an applied field, which is itself similar to the dynamics used to analyze the Ising model by Kawasaki [28]. The dynamics of this simpler, symmetric model has not been researched much, perhaps because the model with the applied field is so interesting; however, it seems that the simple symmetric model exhibits complex unexpected behavior when driven by a chemical potential difference at the boundary. The quantity λ parametrizes the "stickiness" of the particles; when $\lambda > 1$, there is a tendency for particles to repel, whilst $\lambda < 1$ represents attraction. We prove in the supplementary materials that the rates specified in Fig. 1 obey detailed balance, with a Hamiltonian isomorphic to the Ising model.

The SPM model described in Fig. 1 is very simple, but numerical simulation shows that it is capable of a wide range of behaviors, such as those shown in Fig. 4. We will discuss these numerical results in more detail later, but first let us analyze the model behavior using analytic means. Because of the interactions, the types of methods used for the full analytic solution of SEP cannot be applied; thus we pursue a mean field theory approximation.

Let the spacing between lattice sites be a, let τ_0 be the free-particle hopping timescale, and the time-averaged (or ensemble-averaged, assuming ergodicity) occupation probability of the i^{th} lattice site be ρ_i. We introduce

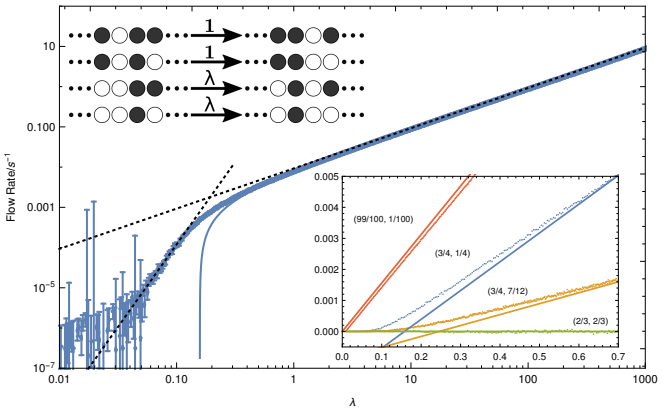

FIG. 1. **Top left:** SPM dynamics: White circles indicate particles, dark circles indicate empty sites (vacancies). Particles randomly move into adjacent vacancies with rate 1, unless there is an adjacent particle, in which case they move with rate λ; the state of the site beyond the new position is irrelevant. Particles can move left or right, such that the whole model is totally symmetric.
Bottom right: Mean flow rate observed as a function of λ with fixed boundary densities (ρ_0, ρ_L) as labeled in the plot. The MFT predictions are indicated by the solid line. Each data point is derive from systems of length 64 (length 32, 128 and 256 give similar results), run for 400000 Gillespie steps for equilibration followed by 10000 measurement runs of 1000 steps interspersed with relaxation runs of 16000 steps. This way we could gather statistics about flow rates and densities in a well-equilibrated system. Specifically, we generate a pool of 10000 samples of flow rate and density from which we can calculate estimates of the descriptive statistics of both quantities; flow moments and the density data are included in the supplementary materials.
Main figure: Log-log plot of the blue $\left(\frac{3}{4}, \frac{1}{4}\right)$ data on the inset plot, extended over a wide range of orders of magnitude of λ. The dashed lines represent power-laws; the higher-λ one is asymptotically matched to the mean-field, diffusion-limit prediction λ^1, whilst the lower-λ one is fitted to the power-law behavior in the range $0.04 \leq \lambda \leq 0.1$: a critically-slowed flow proportional to λ^4.

$\zeta = 1 - \lambda$ here for convenience: high ζ implies sticky particles, negative ζ implies repulsion. One may show that, in the mean-field approximation regime,

$$\tau_0 \frac{\partial \rho_i}{\partial t} = (1-\rho_i)\left[(1-\zeta\rho_{i-2})\,\rho_{i-1} + (1-\zeta\rho_{i+2})\,\rho_{i+1}\right] - \rho_i\left[2\zeta\rho_{i-1}\rho_{i+1} - (3-\zeta)\,(\rho_{i-1}+\rho_{i+1}) + 2\right]. \tag{1}$$

Switching to the continuum limit by taking $a \to 0$, and neglecting $\mathcal{O}(a^4)$ terms, we may re-express this as a conserved flow J as follows:

$$\frac{\partial \rho}{\partial t} = -\frac{\partial J}{\partial x}, \tag{2}$$

$$J = -D(\rho)\frac{\partial \rho}{\partial x}, \tag{3}$$

$$D(\rho) = \frac{a^2}{\tau_0}\left[1 - \zeta\rho\,(4-3\rho)\right]. \tag{4}$$

Thus, the MFT says that the particles should diffuse with a diffusion coefficient $D(\rho)$ which depends upon the local density.

In order to understand the implications of the MFT, let us consider some limits. As $\zeta \to 0$ (i.e. as the model becomes a simple exclusion model), $D \to \frac{a^2}{\tau_0}$. Likewise, in the dilute limit $\rho \to 0$, $D \to \frac{a^2}{\tau_0}$, reflecting the fact that it becomes a dilute lattice gas and therefore the interactions between particles become irrelevant as they never meet. Conversely, in the full limit $\rho \to 1$, $D \to \frac{\lambda a^2}{\tau_0}$; this is because we now have a dilute gas of vacancies, which hop with rate $\frac{\lambda}{\tau_0}$. One may observe that the continuum limit MFT has a symmetry under $\rho \mapsto \frac{4}{3} - \rho$; thus, the dynamics should be symmetric under a density profile reflection around $\rho = \frac{2}{3}$. This is where D always attains its extremal value, $\frac{a^2}{\tau_0}\left[1 - \frac{4}{3}\zeta\right]$, hence for $\zeta > 3/4$ the MFT diffusion coefficient becomes negative in regions with $\frac{2}{3} - \frac{\sqrt{\zeta(4\zeta-3)}}{3\zeta} < \rho < \frac{2}{3} + \frac{\sqrt{\zeta(4\zeta-3)}}{3\zeta}$. Finally, it is possible to show that solutions to the continuum MFT containing domains with a negative diffusion coefficient are linearly unstable; thus, if $D_{MFT}(\rho) < 0$, ρ itself is unstable with respect to either of the two densities for which $D(\rho) \sim 0$. Instead of observing "backwards diffusion" we would see an extremely slow flow or no flow at all. The MFT implies that the transition to this critically slowly-flowing regime happens suddenly, like a phase transition: this can be checked with numerics.

It is possible to solve the continuum MFT in a steady state on a finite domain, say $x \in (0, L)$. The continuity equation implies that $J(x) = J_0 = \text{const.}$, and by integrating both sides of this equation with respect to x we find that

$$J(x) = (x - x_0)J_0 = -\frac{a^2}{\tau_0}\rho\left[1 + \zeta\rho\,(\rho - 2)\right] \tag{5}$$

a cubic equation which can be solved to give $\rho(x)$ with appropriately chosen real constant x_0. If we impose Dirichlet boundary conditions on this system, say $\rho(0) = \rho_0$ and $\rho(L) = \rho_L$, we find that

$$J_0 = \frac{a^2}{L\tau_0}\left[\rho_0 - \rho_L + \zeta\left(\rho_0\left[\rho_0^2 - 2\right] - \rho_L\left[\rho_L^2 - 2\right]\right)\right]. \tag{6}$$

We may consider applying small concentration gradients across a domain by setting $\rho_0 = \rho_M + \frac{1}{2}\delta\rho$ and $\rho_L = \rho_M - \frac{1}{2}\delta\rho$. Doing so, we find that the effective diffusion

coefficient of the domain $D_{\text{Eff}} = L\frac{\partial J}{\partial \delta\rho}\big|_{\delta\rho=0}$ obeys

$$D_{\text{Eff}} = \frac{a^2}{\tau_0}\left[1 - \zeta\rho_M(4 - 3\rho_M)\right], \tag{7}$$

which implies the same symmetry about $\rho = \frac{2}{3}$ and negative flow region as Eq. 4

We also implemented the SPM numerically using the `KMCLib`[29] package, which implements the Kinetic Monte Carlo algorithm (essentially the same as the Gillespie algorithm[30–32]) on lattice systems. The codes used are kept here [33]. In the bulk, the transition rates are simply those described in Fig. 1. With periodic boundary conditions, we recover the fixed magnetization Ising Model, as expected.

To investigate flow, we set up a chemical potential difference across the system by define the boundaries there are 2 layers of lattice sites which switch between being full and empty such that the time-averaged occupation matches the desired concentration; there are then chances for particles to appear and disappear with rates depending upon the occupation of these boundary layers. These boundary conditions should reproduce the effect of having particle reservoirs attached to the edges of the domain, which we verified by inspecting the time-averaged occupations of sites near the boundary.

We have used the setup above to explore three scenarios, discussed in the following sections. In each of these we refer to a boundary condition configuration by (ρ_0, ρ_L), with ρ_0 and ρ_L being the bottom and top boundary densities respectively. We measure overall particle flow rate from the number of particles entering and leaving in a given time. We also maintain a histogram of the distribution of the number of particles in the system. Our initial configurations have randomly distributed particles with density $\frac{1}{2}(\rho_0 + \rho_L)$, and we then run the system for a sufficient number of equilibration steps to destroy any initial transients.

The MFT suggests that a transition from a steady flow regime to a critically slow flow regime might occur as the stickiness varies. We test for this by holding the boundary densities constant whilst changing λ, and measuring the particle density as well as the mean, variance and skewness of the flow rate. If such a transition does indeed occur, we should expect to see something interesting happen as λ passes through the transition point.

The inset in Fig. 1 shows flow rates for a range of λ with four sets of boundary conditions. whilst the main body shows a log-log plot with a single set of boundary conditions over a large range of λ. The equivalent MFT results are shown as a function of λ and $\delta\rho$, since the density within the system $\rho(x)$, obtained by solving the cubic Eq. 5, is non-unique for $\lambda < \frac{1}{4}$. The inset suggests that the SPM flow goes to zero, albeit at lower λ than implied by MFT. However the main figure shows that some flow does continue, at a much reduced rate and with different power-law behavior from particle diffusion. This different flow behavior defines the SPM transition. For low-stickiness ($\lambda > \frac{1}{4}$) the MFT is in very good agreement with the simulations, and this continues for repulsive $\lambda >> 1$, where the mean flow rate varies linearly with λ.

For very high-stickiness $\lambda < 0.04$, convergence is very slow, hence the large standard errors. However, there is a regime when $0.04 \leq \lambda \leq 0.1$ where the mean flow displays clear $\mathcal{O}(\lambda^4)$ power-law behaviour. The SPM transition is where the power laws cross at $\lambda = 0.194$, in good agreement with the MFT switching to negative flow. The key point here is that as that as we pass from high-λ to low-λ, the scaling in λ does change, which suggests to us that the mechanism by which material is transferred through the medium changes from the standard diffusive one (which is well-described by the MFT) to something different, which to our knowledge has not been previously observed.

We also investigate varying both the driving force ($\delta\rho$) and stickiness (λ), using boundaries $(\rho_0, \rho_L) = (\rho_M + \frac{1}{2}\delta\rho, \rho_M - \frac{1}{2}\delta\rho)$ for some given ρ_M. As before, we calculated flow rate moments and average densities (Fig. 2). The MFT prediction for the mean flow is again a good fit until λ becomes sufficiently small, and as before the simulations show no evidence of negative diffusion; rather the flow becomes critically slow for these very sticky particles. The higher moments of the flow (e.g. variance) do not show sharp peaks, again indicating that the transition is a crossover in behaviour. The density within the system is very close to ρ_M until λ drops below 1/4, at which point the system fills ($\rho \sim 1$).

For relatively small driving force $\delta\rho$, we find J varies approximately linearly with $\delta\rho$, thus we can define $D_{\text{Eff}} = \frac{\partial J}{\partial \delta\rho}\big|_{\delta\rho=0}$, the effective diffusion coefficient and measure it using linear regression.

We compare the measured diffusion from (Fig. 3) with the MFT result (Eq. 7) The MFT and simulation agree well for low stickiness, and both show the maximum D at $\rho_M = \frac{2}{3}$. For high stickiness, where the MFT prediction gives negative diffusion constant, measurement gives very low positive values for the current making determination of D difficult, however the important thing to note is that this critically slow flow corresponds to the the negative - D region predicted by the MFT (indicated in purple).

It is instructive to get an overview of how the SPM particles move during flow. Fig. 4 shows a plot of the flow structure in an interesting regime. Over short timescales little structure is visible, the dynamics appearing as a random walk with some tendency for particles to clump; over longer timescales the diffusive behavior is more evident, with a textured structure suggesting characteristic velocity of particles or vacancies through emergent correlated clumps. In the limiting case of low λ the density of particles in the system tends to 1, irrespective of boundary density: this may be because the interactions between particles are strong enough that the filled

FIG. 2. Flow rate mean observed when varying the difference $\delta\rho$ between the boundary concentrations $(\rho_0, \rho_L) = (\rho_M + \frac{1}{2}\delta\rho, \rho_M - \frac{1}{2}\delta\rho)$ and λ (The top panel is the MFT prediction for the flow rate, whilst bottom shows the observed mean flow rate). We chose $\rho_M = \frac{1}{2}$, as this gives us the biggest range of $\delta\rho$ to investigate. These calculations were performed with the same run parameters (system length etc) as above.

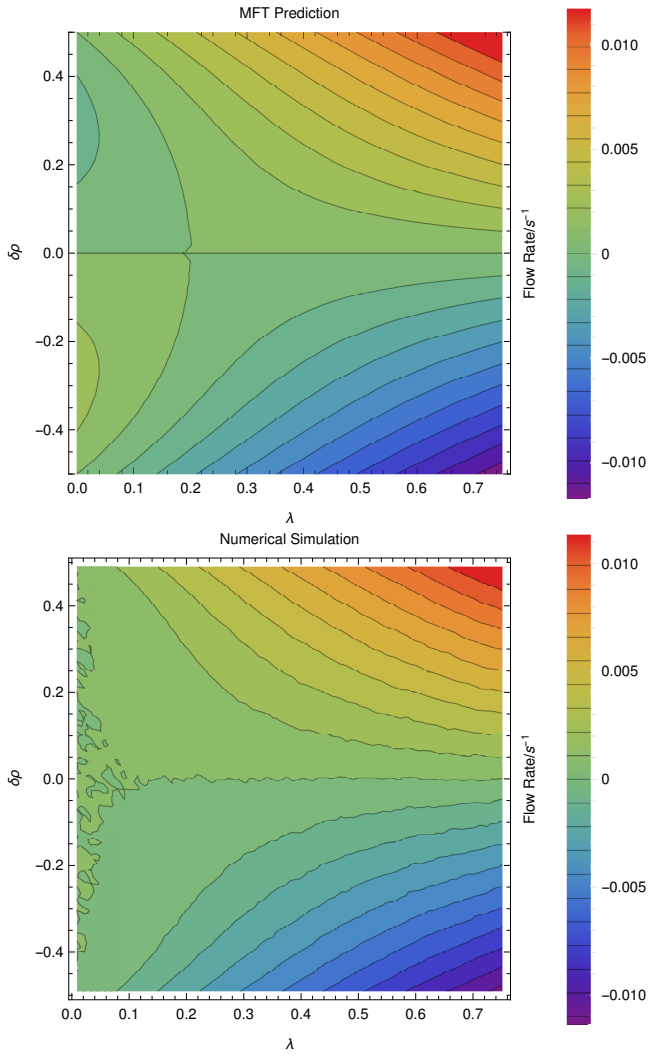

FIG. 3. Comparison of effective diffusion coefficient D in the MFT (top) and in direct simulation (bottom) as a function of density and stickiness. The region where MFT gives negative diffusion is represented as $D = 0$. The simulations used 124 sites averaged over $\sim 10^9$ steps at each of $12 \times 24 \times 16$ $(\lambda, \rho_M, \delta\rho)$ combinations. Full details in the supplementary materials.

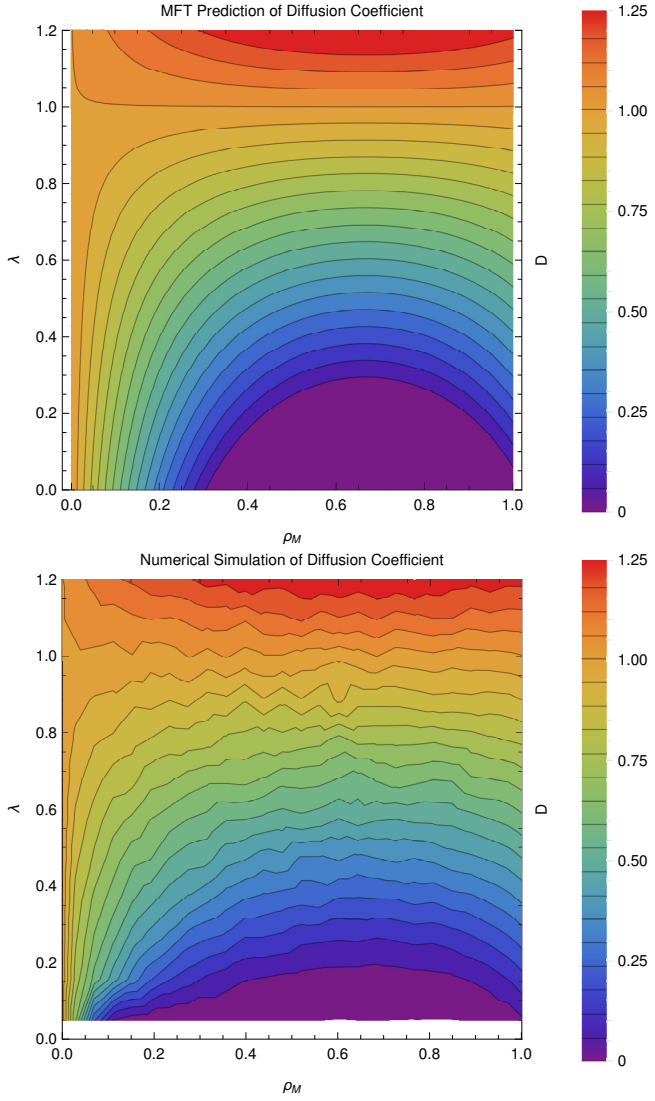

state has lower chemical potential than either boundary. Another interesting case is the limit of high λ, where irrespective of boundary density, the internal density tends to $\rho = \frac{2}{3}$, the value which gives maximal flow. Additional plots can be found in the supplementary materials.

To conclude, we have solved a nonlinear model for self-interacting sticky particles diffusing in 1D. Although only the particles exhibit stickiness, the analytics suggest a symmetry between vacancy-type and particle-type flow at density of $\frac{2}{3}$, which is observed in the simulation. The flow exhibits a foamy pattern with intermediate time-and-space correlations. The continuum solution MFT is a good predictor of the bulk flow behavior of the SPM. The negative diffusion constant found in MFT at high stickiness indicates that the assumption of homogeneous density break down: thus the MFT predicts its own demise, and this agrees well with our numerics.

We would like to thank EPSRC (student grant 1527137) and Wolfson Foundation for providing the funding, Mikael Leetmaa for producing `KMCLib`, and the `Eddie3` team here at Edinburgh for maintaining the hardware used. We would also like to thank Martin Evans, Bartek Waclaw and Richard Blythe for some very helpful discussions during the production of this letter.

FIG. 4. Indicative spacetime flow pattern for sticky free-flow $\left[\lambda = \frac{3}{20}, (\rho_0, \rho_L) = (\frac{3}{4}, \frac{1}{4})\right]$; other combinations shown in the supplementary materials. Time runs along the x-axis, space (1 pixel=1 site) along the y-axis, with grayscale tone (black being empty, white being full) illustrating average site occupation over (clockwise from top left) $\frac{1}{32}$, 1, 8 and 32 Gillespie steps per site respectively.

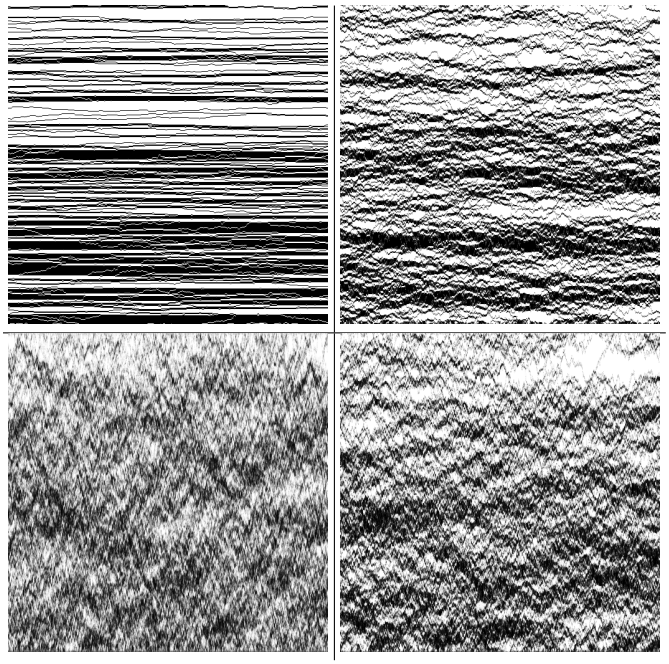

* J.D.M.Hellier@sms.ed.ac.uk
† G.J.Ackland@ed.ac.uk

[1] V. Belitsky and G. M. Schütz, Journal of Statistical Mechanics: Theory and Experiment **2011**, P07007 (2011).
[2] M. Mobilia, I. T. Georgiev, and U. C. Täuber, Journal of Statistical Physics **128**, 447 (2007).
[3] B. Tegner, L. Zhu, C. Siemers, K. Saksl, and G. Ackland, Journal of alloys and compounds **643**, 100 (2015).
[4] L. Zhu, Q.-M. Hu, R. Yang, and G. Ackland, Journal of Physical Chemistry C **116**, 24201 (2012).
[5] B. E. Deal and A. S. Grove, Journal of Applied Physics **36**, 3770 (1965), https://doi.org/10.1063/1.1713945.
[6] N. Cabrera and N. F. Mott, Reports on Progress in Physics **12**, 163 (1949).
[7] S. Buzzaccaro, R. Rusconi, and R. Piazza, Phys. Rev. Lett. **99**, 098301 (2007).
[8] A. J. C. Ladd, M. E. Colvin, and D. Frenkel, Phys. Rev. Lett. **60**, 975 (1988).
[9] T. M. Liggett, *Interacting particle systems* (Springer-Verlag, Berlin, 1985).
[10] E. Ben-Naim, S. Y. Chen, G. D. Doolen, and S. Redner, Phys. Rev. Lett. **83**, 4069 (1999).
[11] S. F. Shandarin and Y. B. Zeldovich, Rev. Mod. Phys. **61**, 185 (1989).
[12] L. Frachebourg, Phys. Rev. Lett. **82**, 1502 (1999).
[13] L. Frachebourg, P. A. Martin, and J. Piasecki, Physica A Statistical Mechanics and its Applications **279**, 69 (2000), cond-mat/9911346.
[14] V. V. Obukhovsky, A. M. Kutsyk, V. V. Nikonova, and O. O. Ilchenko, Phys. Rev. E **95**, 022133 (2017).
[15] N. V. Gorokhova and O. E. Melnik, Fluid Dynamics **45**, 679 (2010).
[16] M. Kardar, G. Parisi, and Y.-C. Zhang, Phys. Rev. Lett. **56**, 889 (1986).
[17] J. Krug and H. Spohn, Phys. Rev. A **38**, 4271 (1988).
[18] T. Sasamoto and H. Spohn, Phys. Rev. Lett. **104**, 230602 (2010).
[19] K. E. P. Sugden and M. R. Evans, Journal of Statistical Mechanics: Theory and Experiment **2007**, P11013 (2007).
[20] M. Kollmann, Phys. Rev. Lett. **90**, 180602 (2003).
[21] B. Lin, M. Meron, B. Cui, S. A. Rice, and H. Diamant, Phys. Rev. Lett. **94**, 216001 (2005).
[22] C. Hegde, S. Sabhapandit, and A. Dhar, Phys. Rev. Lett. **113**, 120601 (2014).
[23] P. L. Krapivsky, K. Mallick, and T. Sadhu, Phys. Rev. Lett. **113**, 078101 (2014).
[24] T. Imamura, K. Mallick, and T. Sasamoto, Phys. Rev. Lett. **118**, 160601 (2017).
[25] S. Katz, J. L. Lebowitz, and H. Spohn, Journal of Statistical Physics **34**, 497 (1984).
[26] R. K. P. Zia, Journal of Statistical Physics **138**, 20 (2010).
[27] Y. Kafri, E. Levine, D. Mukamel, G. M. Schütz, and R. D. Willmann, Phys. Rev. E **68**, 035101 (2003).
[28] K. Kawasaki, Phys. Rev. **145**, 224 (1966).
[29] M. Leetmaa and N. V. Skorodumova, Computer Physics Communications **185**, 2340 (2014), arXiv:1405.1221 [physics.comp-ph].
[30] D. T. Gillespie, The Journal of Physical Chemistry **81**, 2340 (1977), http://dx.doi.org/10.1021/j100540a008.
[31] A. Bortz, M. Kalos, and J. Lebowitz, Journal of Computational Physics **17**, 10 (1975).
[32] A. Prados, J. J. Brey, and B. Sánchez-Rey, Journal of Statistical Physics **89**, 709 (1997).
[33] J. Hellier, (2018), 10.5281/zenodo.1162818.